Bioresource Technology 171 (2014) 10–15

Contents lists available at ScienceDirect

Bioresource Technology

journal homepage: www.elsevier.com/locate/biortech

# Catalytic fast pyrolysis of cellulose and biomass to produce levoglucosenone using magnetic $SO_4^{2-}/TiO_2$–$Fe_3O_4$

Qiang Lu [a,*], Xiao-ning Ye [a], Zhi-bo Zhang [a], Chang-qing Dong [a], Ying Zhang [b]

[a] National Engineering Laboratory for Biomass Power Generation Equipment, North China Electric Power University, Beijing 102206, China
[b] Key Laboratory for Biomass Clean Energy of Anhui Province, University of Science and Technology of China, Hefei 230026, China

## HIGHLIGHTS

- LGO was selectively produced from cellulose and poplar wood using magnetic $SO_4^{2-}/TiO_2$–$Fe_3O_4$.
- Catalytic temperature and feedstock/catalyst ratio affected the pyrolytic product distribution greatly.
- The LGO yields reached 15.43 wt% from cellulose and 7.06 wt% from poplar wood.
- The $SO_4^{2-}/TiO_2$–$Fe_3O_4$ performed better than the $SO_4^{2-}/TiO_2$, $H_3PO_4$ and $H_2SO_4$ to produce LGO.

## ARTICLE INFO

*Article history:*
Received 28 July 2014
Received in revised form 14 August 2014
Accepted 17 August 2014
Available online 23 August 2014

*Keywords:*
Levoglucosenone
Catalytic fast pyrolysis
Magnetic superacid catalyst
Cellulose
Biomass

## ABSTRACT

Magnetic superacid ($SO_4^{2-}/TiO_2$–$Fe_3O_4$) was prepared for catalytic fast pyrolysis of cellulose and poplar wood to produce levoglucosenone (LGO). Its catalytic activity was evaluated via pyrolysis–gas chromatography/mass spectrometry (Py–GC/MS) experiments, and compared with the non-magnetic $SO_4^{2-}/TiO_2$, phosphoric acid ($H_3PO_4$) and sulfur acid ($H_2SO_4$) catalysts. Moreover, the LGO yield was quantitatively determined. The results indicated that the magnetic $SO_4^{2-}/TiO_2$–$Fe_3O_4$ was effective to selectively produce LGO from both cellulose and poplar wood. Its catalytic capability was a little better than the non-magnetic $SO_4^{2-}/TiO_2$ and $H_3PO_4$, and much better than the $H_2SO_4$. The maximal LGO yields from both cellulose and poplar wood were obtained at 300 °C with the feedstock/catalyst ratio of 1/1, reaching as high as 15.43 wt% from cellulose and 7.06 wt% from poplar wood, respectively.



## 1. Introduction

Selective pyrolysis of biomass to produce specific valuable chemicals is a new and promising way for the value-added utilization of biomass materials, and has gained extensive attention in recent years (Mohan et al., 2006; Huang et al., 2012; Zhang et al., 2013; Bu et al., 2014). LGO is one of the valuable chemicals that can be selectively produced. It is an anhydrosugar product derived from the depolymerization and dehydration of cellulose (Halpern et al., 1973; Ohnishi et al., 1975). Due to its unique structure, LGO has been regarded as a promising building block with high versatility in modern organic synthesis, to prepare various bioactive compounds, disaccharides, chiral inductors, and so on (Sarotti et al., 2012).

LGO is usually a minor pyrolytic product from cellulose or biomass (Lu et al., 2011b), but its yield can be increased remarkably in some acid-catalyzed pyrolysis processes (Di Blasi et al., 2008; Lu et al., 2011a). Catalyst is the key factor that determines the LGO yield, and thus, it is very important to study and find out promising catalysts to achieve high selective LGO production. Till now, five catalysts have been reported to have high catalytic selectivity on the LGO formation, including $H_3PO_4$ (Dobele et al., 2003, 2005; Sarotti et al., 2007; Nowakowski et al., 2008; Zandersons et al., 2013), $H_2SO_4$ (Branca et al., 2011; Sui et al., 2012), $Fe_2(SO_4)_3$ (Dobele et al., 2005), solid superacid ($SO_4^{2-}/TiO_2$ or $SO_4^{2-}/ZrO_2$) (Wang et al., 2011b; Lu et al., 2012; Wei et al., 2014) and 1-butyl-2,3-dimethylimidazolium triflate ionic liquid (Kudo et al., 2011). Among these catalysts, the $H_3PO_4$, $Fe_2(SO_4)_3$ and $H_2SO_4$ catalysts should be impregnated on the cellulose/biomass, which requires complex pretreatment process. Moreover, the $H_3PO_4$ and $H_2SO_4$ would undergo thermal condensation reactions during the pyrolysis process, making their recycle impossible. Nevertheless, the solid superacid catalysts are easy to utilize, by just mechanically mixing with the cellulose/biomass, which will offer significant advantage on feedstock pretreatment. They are also thermally stable, and thus,

* Corresponding author. Tel.: +86 10 61772063; fax: +86 10 61772032(801).
*E-mail address:* qianglu@mail.ustc.edu.cn (Q. Lu).

http://dx.doi.org/10.1016/j.biortech.2014.08.075
0960-8524/

can be recycled. However, how to recycle the catalyst is an important problem for the industrial process, since the catalyst will be mixed with the solid char residues after the catalytic pyrolysis process.

To facilitate the catalyst recycles, magnetic sold superacid catalyst ($SO_4^{2-}/TiO_2$–$Fe_3O_4$) was prepared in this study. Its catalytic activity was evaluated via the Py–GC/MS technique which was a powerful tool for primary catalyst selection and evaluation. Currently, solid superacid catalysts have only been employed for the LGO production from cellulose. In this study, both cellulose and poplar wood were employed as the feedstock for selective production of LGO using $SO_4^{2-}/TiO_2$–$Fe_3O_4$. The catalytic capabilities of the magnetic $SO_4^{2-}/TiO_2$–$Fe_3O_4$ were compared with the non-magnetic $SO_4^{2-}/TiO_2$ as well as the previously reported $H_3PO_4$ and $H_2SO_4$ catalysts. Moreover, the LGO yields from different reaction conditions were quantitatively determined.

## 2. Experimental

### 2.1. Materials

The feedstock used in this study included microcrystalline cellulose (Avicel PH-101), poplar wood and pure LGO. The microcrystalline cellulose and pure LGO were purchased from Sigma and TCI company, respectively. Prior to experiments, the poplar wood was ground in a high speed rotary cutting mill, and screened using two standard sieves to obtain the particles within the size of 0.2–0.3 mm. The particles were then dried in an oven at 110 °C for 3 h in air, and stored in a vacuum desiccator (containing silica gel in it and in a vacuum condition with the pressure lower than 2 kPa) at room temperature for experiments. Its chemical composition was analyzed according to Ranganathan et al. (1985), and its elemental composition on the dry basis was analyzed by an Elementar vario MACRO cube analyzer.

### 2.2. Preparation of the $TiO_2$, $SO_4^{2-}/TiO_2$ and $SO_4^{2-}/TiO_2$–$Fe_3O_4$ catalysts

The $TiO_2$ was prepared by the following procedure. Certain amount of $TiCl_4$ was slowly added to deionized water with vigorous stirring and cooled by ice water. NaOH solution (0.1 mol/L) was then added dropwise to the above mixture to a final pH around 8. The precipitate was filtered, washed with deionized water until no chloride ions (tested by 1 mol/L $AgNO_3$ solution), and dried at 110 °C for 24 h. The obtained solids ($Ti(OH)_4$) were powdered below 100 mesh, and some solids were used for the preparation of the $SO_4^{2-}/TiO_2$ and $SO_4^{2-}/TiO_2$–$Fe_3O_4$. The other solids were calcined at 550 °C for 3 h to obtain the $TiO_2$.

The $SO_4^{2-}/TiO_2$ (non-magnetic solid superacid) was prepared by the impregnation of the above $Ti(OH)_4$ with 1 mol/L aqueous sulfuric acid under stirring for 12 h. Afterwards, the mixture was filtered, wash with deionized water until no sulfate ions (tested by 1 mol/L $BaCl_2$ solution), dried at 110 °C for 24 h, and finally calcined at 550 °C for 3 h to obtain the $SO_4^{2-}/TiO_2$.

To prepare the $SO_4^{2-}/TiO_2$–$Fe_3O_4$ (magnetic solid superacid), the magnetic substrate was firstly produced. 6 g $FeCl_3{\cdot}6H_2O$ and 2 g $FeCl_2{\cdot}4H_2O$ were dissolved in 40 mL and 18 mL deionized water, and then mixed together. Afterwards, NaOH solution (0.1 mol/L) was added into the above solution to a final pH of 10–11 with stirring for 30 min. The mixture was then placed above a magnet for 12 h to achieve separation by the magnetic field. The obtained solid was washed with deionized water until the pH was neutral, and dried at 105 °C for 24 h to obtain the magnetic substrate. The $SO_4^{2-}/TiO_2$–$Fe_3O_4$ was prepared with the following procedure.1 g polyethylene glycol was added to 300 mL deionized water, followed with the slow addition of 12 mL $TiCl_4$ and 0.5 g magnetic substrate, under vigorous stirring and cooled by ice water. NaOH solution (0.1 mol/L) was then added dropwise to the above mixture to a final pH around 8. The precipitate was filtered, washed with deionized water until no chloride ions (tested by 1 mol/L $AgNO_3$ solution), and dried at 110 °C for 24 h. The obtained solids were powdered below 100 mesh, and impregnated with 1 mol/L aqueous sulfuric acid under stirring for 12 h. The mixture was filtered, washed with deionized water until no sulfate ions (tested by 1 mol/L $BaCl_2$ solution), dried at 110 °C for 24 h, and finally calcined at 550 °C for 3 h to obtain the $SO_4^{2-}/TiO_2$–$Fe_3O_4$.

### 2.3. Catalyst characterization

The catalysts were characterized via the X-ray diffraction (XRD) analysis, Fourier transform infrared (FTIR) analysis, textural property analysis, sulfur content analysis and magnetic property analysis. The XRD analysis was performed with a Philips X'pert PRO X-ray diffractometer, employing the Cu $K_\alpha$ radiation ($\lambda = 0.15418$ nm). The data were recorded over the $2\theta$ range of 10–90°. The FTIR analysis was conducted using a Perkin Elmer spectrophotometer. Nitrogen adsorption/desorption isotherms at 77 K of the catalysts were measured using an Autosorb-iQ-MP physisorption analyzer. The surface areas were determined using the Brunauer–Emmett–Teller (BET) method, and the pore volumes were determined by the Barrett–Joyner–Halenda (BJH) method. The sulfur contents of the $SO_4^{2-}/TiO_2$ and $SO_4^{2-}/TiO_2$–$Fe_3O_4$ catalysts were determined by an Elementar vario MACRO cube analyzer. The magnetic property of the $SO_4^{2-}/TiO_2$–$Fe_3O_4$ catalyst was characterized using a LakeShore 7407 series vibration sample magnetometer (VSM).

### 2.4. Pretreatment of the cellulose with $H_3PO_4$ and $H_2SO_4$

$H_3PO_4$ and $H_2SO_4$ catalysts were previously reported to be effective for selective production of LGO. In order to compare their catalytic capability with the $SO_4^{2-}/TiO_2$–$Fe_3O_4$ and $SO_4^{2-}/TiO_2$ catalysts, the cellulose was pretreated to impregnate the $H_3PO_4$ or $H_2SO_4$ using the incipient wetness impregnation method (Zhang et al., 2014). Aqueous $H_3PO_4$ or $H_2SO_4$ solutions (3 mL) with different concentrations were prepared and then added to 1 g cellulose with ultrasonic treatment for 12 h. Afterwards, the mixtures were dried at 105 °C for 3 h and stored in a desiccator for experiments. A total of twelve pretreated cellulose samples were prepared, with the $H_3PO_4$ or $H_2SO_4$ contents of 2.5, 5.0, 7.5, 10.0, 15.0 and 20.0 wt%, respectively.

### 2.5. Py–GC/MS experiments

Pyrolysis was performed using the CDS Pyroprobe 5200HP pyrolyser (Chemical Data Systems). Five catalysts were tested to evaluate the catalytic capabilities on the LGO production from either cellulose or poplar wood, including three solid catalysts ($SO_4^{2-}/TiO_2$–$Fe_3O_4$, $SO_4^{2-}/TiO_2$, $TiO_2$) and two liquid catalysts ($H_3PO_4$ and $H_2SO_4$). To evaluate the solid catalysts, 0.20 mg cellulose (or poplar wood) and certain amounts of solid catalyst (0.05, 0.10, 0.20, 0.40 or 0.80 mg) were filled in the quartz tube and mechanically mixed together. To evaluate the liquid catalysts, certain quantities of the pretreated cellulose samples were filled in the quartz tube. The quantities were strictly weighed to be 0.21, 0.21, 0.22, 0.22, 0.24 and 0.25 mg for the samples impregnated with 2.5, 5.0, 7.5, 10.0, 15.0 and 20.0 wt% $H_3PO_4$ or $H_2SO_4$, to ensure the pure cellulose quantity of each sample strict to be 0.20 mg. An analytical balance with the readability of 0.01 mg was used for weighing. The sample preparation details can be found in our previous studies (Lu et al., 2011a, 2012).

The pyrolysis was carried out in the temperature range of 250–450 °C for 20 s with the heating rate of 20 °C/ms. The pyrolysis

vapors were directly transferred to the Perkin Elmer GC/MS (Clarus 560) and analyzed by it. The injector temperature was kept at 300 °C. An Elite-35MS capillary column (30 m × 0.25 mm i.d., 0.25 μm film thickness) was used for the chromatographic separation. Helium (99.999%) was used as the carrier gas with a constant flow rate of 1 mL/min and a 1:80 split ratio. The oven temperature was programmed from 40 °C (2 min) to 280 °C at the heating rate of 15 °C/min. The temperature of the GC/MS interface was held at 280 °C, and the mass spectrometer was operated in EI mode at 70 eV. The chromatographic peaks were identified according to the NIST library, Wiley library and the literature data of previous reports.

For each sample, the experiments were conducted at least three times. For each pyrolytic product, its peak area and peak area% values were recorded, and the average and standard deviation values were calculated and used for analysis. The Py–GC/MS technique could not provide the direct quantitative analysis of the pyrolytic products. However, it is known that the chromatographic peak area of a product is considered to vary linearly with its quantity, and the peak area% is considered to vary linearly with its content. Therefore, for each product, the changes of its yield can be determined by comparing its average peak area values obtained at different pyrolysis conditions, and the changes of its relative content among the detected products can be determined by comparing its average peak area% values.

### 2.6. Quantitative determination of the LGO yield

Quantitative determination of the LGO yield was performed using an external standard method. Different amounts of pure LGO were directly subjected to Py–GC/MS experiments, the LGO was the only compound detected by GC/MS, and its peak area values were recorded. Hence, a straight line was obtained in terms of the LGO quantity and its chromatographic peak area. Based on this line and the original feedstock quantity (0.20 mg), it is able to calculate the LGO yield in the analytical Py–GC/MS experiments. To confirm this external standard method, the pure LGO was directly injected to GC/MS to obtain another line in terms of the LGO quantity and its chromatographic peak area. The two lines were almost the same, which confirmed the validity of the external standard method.

## 3. Results and discussion

### 3.1. Catalyst properties

The XRD patterns of $TiO_2$, $SO_4^{2-}/TiO_2$ and $SO_4^{2-}/TiO_2$–$Fe_3O_4$ catalysts are given in the Supplementary Data (Fig. S1). The $TiO_2$ exhibited typical diffraction peaks attributed to the anatase phase reflections. The $SO_4^{2-}/TiO_2$ and $SO_4^{2-}/TiO_2$–$Fe_3O_4$ retained the anatase phase of the parent $TiO_2$, suggesting the $TiO_2$ structure was not altered during the post-treatment process. The FTIR spectra of the three catalysts are also shown in the Supplementary Data (Fig. S2). The spectra of the $SO_4^{2-}/TiO_2$ and $SO_4^{2-}/TiO_2$–$Fe_3O_4$ showed characteristic peaks of the sulfated metal oxides between 900 and 1400 $cm^{-1}$, assigned to the stretching vibrations of the S=O bond or S–O bond (Guo et al., 1994). The $Ti^{4+}$ cation could become a strong acid site due to the strong inductive effect of the S=O bond. The textural properties, sulfur content and magnetic property of the catalysts are shown in Table 1. The $SO_4^{2-}/TiO_2$ and $SO_4^{2-}/TiO_2$–$Fe_3O_4$ possessed a little lower BET surface areas, but higher pore volumes than those of the $TiO_2$.

### 3.2. Production of LGO from catalytic fast pyrolysis of cellulose and poplar wood with $SO_4^{2-}/TiO_2$–$Fe_3O_4$

The chemical and elemental composition results of the poplar wood are given in the Supplementary Data (Table S1). The non-catalytic analytical fast pyrolysis of cellulose and poplar wood has been reported in our previous studies (Lu et al., 2011b; Dong et al., 2012). The typical ion chromatograms are shown in the Supplementary Data (Figs. S3(a) and S3(c)). Pure cellulose has good thermal stability, and during its fast pyrolysis, minor pyrolytic products were firstly detected at the set temperature of 300 °C. Among the pyrolytic products, levoglucosan (LG) was the predominant one, formed via the depolymerization of cellulose (Shen and Gu, 2009; Wang et al., 2012). LGO was a very minor product, formed via the combined depolymerization and dehydration of cellulose. When the $SO_4^{2-}/TiO_2$–$Fe_3O_4$ or $SO_4^{2-}/TiO_2$ catalysts were added into cellulose, the initial devolatilization temperature of the cellulose was lowered, because the pyrolytic products were firstly detected at 250 °C. Moreover, the pyrolytic product distribution was altered greatly by the catalysts, with the typical ion chromatogram shown in the Supplementary Data (Fig. S3(b)). LGO became the major product, together with the furfural (FF), 1,4:3,6-dianhydro-α-D-glucopyranose (DGP), 1-hydroxy-3,6-dioxabicyclo[3.2.1]octan-2-one (LAC), 5-hydromethyl-furfural (HMF) and 1,5-anhydro-4-deoxy-D-glycero-hex-1-en-3-ulose (APP) as by-products. The results clearly indicated that the $SO_4^{2-}/TiO_2$–$Fe_3O_4$ catalyst was capable to significantly promote the LGO formation pathway, and meanwhile inhibit the pathways to form LG and other products.

During fast pyrolysis of pure poplar wood, the pyrolytic products were firstly detected at 300 °C, mainly including hemicellulose-derived pyrolytic products, due to the thermal instability of hemicellulose. The products from higher temperatures mainly included various light linear carbonyls (hydroxyacetaldehyde (HAA), etc.), linear acids (acetic acid (AA), etc.), furan compounds (FF, HMF, etc.) and anhydrosugars (LG, etc.) which were mainly derived from holocellulose, as well as various phenolic compounds which were mainly derived from lignin (Dong et al., 2012). In the presence of catalyst, the product distribution was also changed significantly. LGO was also formed as the major product, together with AA, FF, LAC, DGP, HMF and APP as by-products, as shown in the Supplementary Data (Fig. S3(d)). Compared with the catalytic pyrolytic products from cellulose, more AA and FF were formed in the catalytic pyrolytic products of poplar wood, which were mainly derived from the hemicellulose of the poplar wood (Lu et al., 2011a).

The $SO_4^{2-}/TiO_2$–$Fe_3O_4$ and $SO_4^{2-}/TiO_2$ exhibited similar catalytic capabilities to selectively produce LGO from cellulose and poplar wood. However, the pure $TiO_2$ did not show such catalytic effects, indicating the strong acidity of the $SO_4^{2-}/TiO_2$–$Fe_3O_4$ and $SO_4^{2-}/TiO_2$ was essential for the LGO formation.

#### 3.2.1. Effects of the catalytic temperature

Fig. 1 shows the effects of the catalytic temperature (250–450 °C) on the peak area and peak area% of LGO at the feedstock/catalyst ratio of 1/1. The results from the non-catalytic pyrolysis of cellulose and poplar wood are also presented in Fig. 1 for comparison. During the fast pyrolysis of cellulose, the catalytic effects of the three catalysts ($TiO_2$, $SO_4^{2-}/TiO_2$ and $SO_4^{2-}/TiO_2$–$Fe_3O_4$) were all investigated in details (Fig. 1(a) and (b)). Whereas, during the fast pyrolysis of poplar wood, only $SO_4^{2-}/TiO_2$–$Fe_3O_4$ was subjected to detailed evaluation at all reaction conditions (Fig. 1(c)). The catalytic effects of the $TiO_2$ and $SO_4^{2-}/TiO_2$ were only performed at several key conditions, and their results are not shown here. Moreover, it is to note that the LGO yield from the non-catalytic fast pyrolysis of poplar wood was very low, resulting in very small values of pure poplar wood in Fig. 1(c).

According to Fig. 1, LGO was a very minor product in the non-catalytic or $TiO_2$-catalyzed processes. Whereas, both the peak area and peak area% of the LGO were increased significantly in the catalytic process using $SO_4^{2-}/TiO_2$–$Fe_3O_4$ or $SO_4^{2-}/TiO_2$. Specially, the LGO peak area, which was proportional to its yield, was initially

**Table 1**
Textural properties, sulfur content and magnetic property of the catalysts.

| | BET surface area ($m^2/g$) | Pore volume ($cm^3/g$) | Sulfur content (wt%) | Saturation magnetization (emu) |
|---|---|---|---|---|
| $TiO_2$ | 130.3 | 0.33 | – | – |
| $SO_4^{2-}/TiO_2$ | 115.3 | 0.55 | 3.31 | – |
| $SO_4^{2-}/TiO_2$–$Fe_3O_4$ | 102.6 | 0.45 | 3.10 | 11.7 |

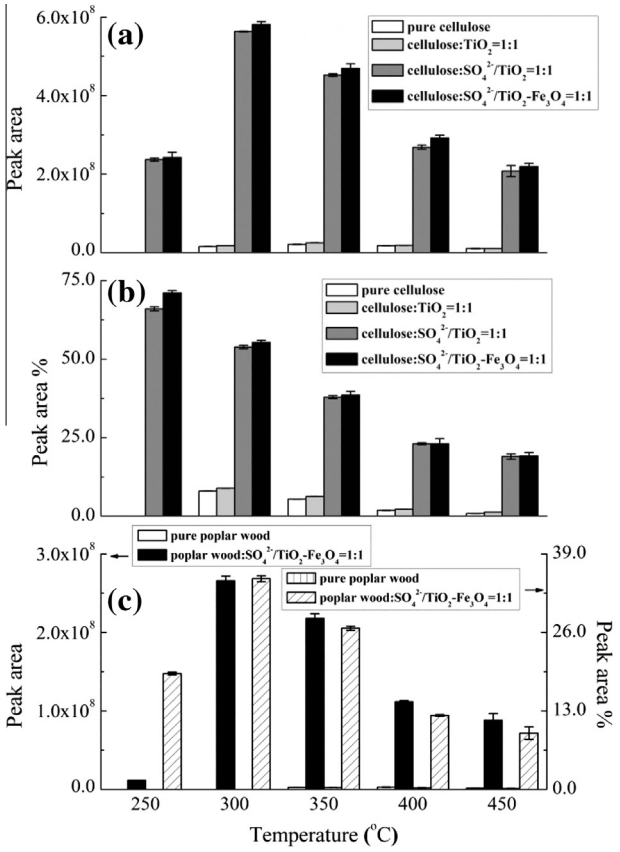


**Fig. 1.** Peak area and peak area% of the LGO from non-catalytic and catalytic fast pyrolysis of cellulose or poplar wood at different temperatures.

increased and then decreased as the catalytic temperature increased. The maximal LGO yields were obtained at 300 °C for both cellulose and poplar wood, and the peak area values were about 32 times or 104 times more than the highest peak area values in the non-catalytic pyrolysis of the cellulose or poplar wood, respectively. Furthermore, the LGO peak area%, which was proportional to its concentration, was decreased monotonically along with the catalytic pyrolysis temperature for cellulose, with the values of 71.1% and 55.5% at 250 and 300 °C, respectively. Moreover, the LGO peak area% was initially increased and then decreased along with the temperature for poplar wood, with the maximal value of 34.9% at 300 °C. The above results indicated that the low pyrolysis temperature was favorable for selective LGO production, agreed well with previous results (Fabbri et al., 2007; Lu et al., 2012; Wei et al., 2014). High pyrolysis temperature (>300 °C) would enhance other competing pyrolytic pathways, and also partly cause the secondary conversion of the LGO, resulting in the decreased LGO production.

Based on Fig. 1, the $SO_4^{2-}/TiO_2$–$Fe_3O_4$ performed a little better than the $SO_4^{2-}/TiO_2$ on the selective LGO production. This observation suggested that the presence of $Fe_3O_4$ in $SO_4^{2-}/TiO_2$–$Fe_3O_4$ would not only act as the magnetic matrix, but also affect the catalytic capability in positive way. Further studies are required to reveal how the $Fe_3O_4$ influenced the catalytic capability of the $SO_4^{2-}/TiO_2$–$Fe_3O_4$.

Besides the LGO, the other pyrolytic products from cellulose and poplar wood were also affected by the catalytic temperature. The results are shown in the Supplementary Data (Fig. S4 and S5). Generally, during the catalytic pyrolysis of cellulose, the LG was significantly decreased as compared with the non-catalytic process, while the FF and DGP were increased. As the rising of the catalytic temperature, the yields of the FF, LAC and LG were gradually increased, indicating their formation was favored at medium temperatures (Fabbri et al., 2007; Lu et al., 2011b). While the yields of the DGP, HMF and APP were initially increased and then decreased, suggesting their formation was favorable at low temperatures (Lu et al., 2011b). It is to note that the DGP could be the precursor of the LGO under the acid-catalyzed pyrolysis process (Shafizadeh et al., 1978), while the LAC was generated from the APP (Furneaux et al., 1988). During the catalytic pyrolysis of the poplar wood, the AA and FF were the two major by-products. The AA yield was similar in the non-catalytic and catalytic processes of different temperatures. The results indicated that the formation of the AA (deacetylation of hemicellulose) would not be greatly influenced by the catalyst and pyrolysis temperature. The FF yield was increased greatly as compared with the non-catalytic process, and it was also gradually increased as the rising of the temperature.

### 3.2.2. Effects of feedstock/catalyst ratio

Fig. 2 gives the peak area and peak area% results of the LGO from the non-catalytic and catalytic processes with the feedstock/catalyst ratios of 1/0.25, 1/0.5, 1/1, 1/2 and 1/4, under the pyrolysis temperature of 300 °C. As the rising of the feedstock/catalyst ratio, the LGO yield and its relative content were initially increased and then decreased. The maximal values were obtained at the feedstock/catalyst ratio of 1/1 for both cellulose and poplar wood. At the low catalyst quantity, the contact of the feedstock and the catalyst was insufficient due to the motionless feedstock/catalyst mixture, resulting in the insufficient catalytic effects to promote the LGO formation. Whereas at high catalyst quantity, the strong acidity of the catalyst would significantly enhance the dehydration and charring of the cellulose or poplar wood, resulting in the decrease of the overall organic volatile products (Branca et al., 2011; Lu et al., 2011a). Moreover, the strong acidic catalyst would also catalyze the secondary conversion of the LGO (Shafizadeh and Chin, 1976). As a result, the LGO yield was decreased remarkably at high catalyst quantity.

### 3.3. Comparison of the catalytic effects of the $SO_4^{2-}/TiO_2$–$Fe_3O_4$, $SO_4^{2-}/TiO_2$, $H_3PO_4$ and $H_2SO_4$

The $H_3PO_4$ and $H_2SO_4$ were previously reported to be effective for selective production of LGO from cellulose. In order to compare their catalytic capability with the $SO_4^{2-}/TiO_2$–$Fe_3O_4$ and $SO_4^{2-}/TiO_2$ catalysts, $H_3PO_4$-impregnated and $H_2SO_4$-impregnated cellulose samples were prepared and subjected to Py–GC/MS experiments. The results revealed that the highest LGO yields were obtained from the cellulose samples with 10.0 wt% $H_3PO_4$ or 5.0 wt% $H_2SO_4$, at the pyrolysis temperature of 300 °C. Therefore, the

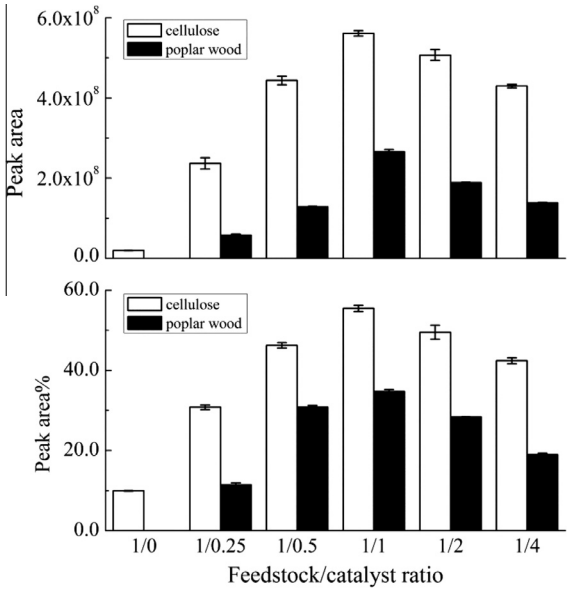


**Fig. 2.** Peak area and peak area% of the LGO under different feedstock/catalyst ratios.

catalytic capability of the four catalysts could be compared, as given in the Supplementary Data (Fig. S6). According to the results, the $H_3PO_4$, $SO_4^{2-}/TiO_2$ and $SO_4^{2-}/TiO_2$–$Fe_3O_4$ catalysts all performed much better than the $H_2SO_4$ to enhance the LGO formation, because the LGO peak area values from the three catalysts were all at least 1.7 times higher than that from the $H_2SO_4$. Among the four catalysts, the $SO_4^{2-}/TiO_2$–$Fe_3O_4$ catalyst exhibited the best catalytic capability on the LGO. Furthermore, the $SO_4^{2-}/TiO_2$–$Fe_3O_4$ catalyst would be easy to utilize and recycle as compared with the other catalysts. These facts all indicated that the $SO_4^{2-}/TiO_2$–$Fe_3O_4$ catalyst should be a promising catalyst for LGO production with low cost.

### 3.4. Quantitative determination of the LGO

The Py–GC/MS technique could not quantitatively analyze the pyrolytic products. Hence, an external standard method was employed to determine the LGO yield. The results are shown in Table 2. Under the catalysis of the $SO_4^{2-}/TiO_2$–$Fe_3O_4$, the highest LGO yields were 15.43 wt% from cellulose and 7.06 wt% from poplar wood, obtained at the pyrolysis temperature of 300 °C and feedstock/catalyst ratio of 1/1. It is clear the LGO yields from cellulose by using the other three catalysts were all lower than that from using the $SO_4^{2-}/TiO_2$–$Fe_3O_4$.

The cellulose content in the poplar wood was 49.0 wt%, and the highest LGO yield from the poplar wood was around 45.7% (calculated by 7.06/15.43) of that from the cellulose. This suggested that the pyrolytic formation of LGO from cellulose in the poplar wood would only be slightly inhibited by the other poplar wood components (hemicellulose, lignin, extractive and ash). It is well known that during fast pyrolysis of biomass, the pyrolytic pathways and product distribution of each component would be affected by the other components (Wang et al., 2011a). Moreover, during the catalytic fast pyrolysis of biomass, the contact between the cellulose of biomass and the catalyst would be partly hindered by the other biomass components. Furthermore, according to the Zandersons et al. (2013) who investigated the effects of biomass pretreatment on the $H_3PO_4$-catalyzed pyrolysis of biomass, the changes of the lignin and hemicellulose contents would clearly influence the LGO formation. All the above facts suggested that the catalytic pyrolysis of biomass using $SO_4^{2-}/TiO_2$–$Fe_3O_4$ to produce LGO might not only be influenced by the catalyst but also the biomass components. Therefore, further studies are required to reveal how the biomass components affected the LGO formation during the catalytic fast pyrolysis of biomass using $SO_4^{2-}/TiO_2$–$Fe_3O_4$, so as to optimize the LGO production from biomass.

**Table 2**
Quantitative determination of the LGO yields from different catalysts and feedstocks (wt%).

| | $H_2SO_4$ | $H_3PO_4$ | $SO_4^{2-}/TiO_2$ | $SO_4^{2-}/TiO_2$–$Fe_3O_4$ |
|---|---|---|---|---|
| Cellulose | 8.53 | 14.92 | 14.95 | 15.43 |
| Poplar wood | | | 6.82 | 7.06 |

## 4. Conclusions

Magnetic $SO_4^{2-}/TiO_2$–$Fe_3O_4$ was prepared and employed for catalytic fast pyrolysis of cellulose and poplar wood to selectively produce LGO. The results indicated that both the catalytic temperature and feedstock/catalyst ratio played important roles on the pyrolytic product distribution. Low catalytic temperature favored the LGO formation. The highest LGO yields reached 15.43 wt% from cellulose or 7.06 wt% from poplar wood, obtained at 300 °C with the feedstock/catalyst ratio of 1/1. Moreover, the catalytic performance of the magnetic $SO_4^{2-}/TiO_2$–$Fe_3O_4$ was compared with the non-magnetic $SO_4^{2-}/TiO_2$, $H_3PO_4$ and $H_2SO_4$, and the $SO_4^{2-}/TiO_2$–$Fe_3O_4$ exhibited the best capability to selectively produce LGO.

## Acknowledgements

The authors thank the National Natural Science Foundation of China (51106052), National Basic Research Program of China (2013CB228103), National Torch Plan (2013GH561645), 111 Project (B12034), and Fundamental Research Funds for the Central Universities (2014ZD17) for financial support.

## Appendix A. Supplementary data

Supplementary data associated with this article can be found, in the online version, at http://dx.doi.org/10.1016/j.biortech.2014.08.075.

## References

Branca, C., Galgano, A., Blasi, C., Esposito, M., Di Blasi, C., 2011. $H_2SO_4$-catalyzed pyrolysis of corncobs. Energy Fuel 25, 359–369.
Bu, Q., Lei, H., Wang, L., Wei, Y., Zhu, L., Zhang, X., Liu, Y., Yadavalli, G., Tang, J., 2014. Bio-based phenols and fuel production from catalytic microwave pyrolysis of lignin by activated carbons. Bioresour. Technol. 162, 142–147.
Di Blasi, C., Branca, C., Galgano, A., 2008. Products and global weight loss rates of wood decomposition catalyzed by zinc chloride. Energy Fuel 22, 663–670.
Dobele, G., Dizhbite, T., Rossinskaja, G., Telysheva, G., Meier, D., Radtke, S., Faix, O., 2003. Pre-treatment of biomass with phosphoric acid prior to fast pyrolysis: a promising method for obtaining 1,6-anhydrosaccharides in high yields. J. Anal. Appl. Pyrol. 68–69, 197–211.
Dobele, G., Rossinskaja, G., Dizhbite, T., Telysheva, G., Meier, D., Faix, O., 2005. Application of catalysts for obtaining 1,6-anhydrosaccharides from cellulose and wood by fast pyrolysis. J. Anal. Appl. Pyrol. 74, 401–405.
Dong, C.Q., Zhang, Z.F., Lu, Q., Yang, Y.P., 2012. Characteristics and mechanism study of analytical fast pyrolysis of poplar wood. Energy Convers. Manage. 57, 49–59.
Fabbri, D., Torri, C., Mancini, I., 2007. Pyrolysis of cellulose catalysed by nanopowder metal oxides: production and characterisation of a chiral hydroxylactone and its role as building block. Green Chem. 9, 1374–1379.
Furneaux, R.H., M.Mason, J., J.Miller, I., 1988. A novel hydroxylactone from the Lewis acid catalyzed pyrolysis of cellulose. J. Chem. Soc., Perkin Trans. 1, 49–51.
Guo, C., Yao, S., Cao, J., Qian, Z., 1994. Alkylation of isobutane with butenes over solid superacids, $SO_4^{2-}/ZrO_2$ and $SO_4^{2222}/TiO_2$. Appl. Catal. A: Gen. 107, 229–238.
Halpern, Y., Riffer, R., Broido, A., 1973. Levoglucosenone (1,6-anhydro-3,4-dideoxy-β-D-pyranosen-2-one). A major product of the acid-catalyzed pyrolysis of cellulose and related carbohydrates. J. Org. Chem. 38, 204–209.

Huang, W., Gong, F., Fan, M., Zhai, Q., Hong, C., Li, Q., 2012. Production of light olefins by catalytic conversion of lignocellulosic biomass with HZSM-5 zeolite impregnated with 6 wt.% lanthanum. Bioresour. Technol. 121, 248–255.

Kudo, S., Zhou, Z., Norinaga, K., Hayashi, J., 2011. Efficient levoglucosenone production by catalytic pyrolysis of cellulose mixed with ionic liquid. Green Chem. 13, 3306–3311.

Lu, Q., Dong, C.Q., Zhang, X.M., Tian, H.Y., Yang, Y.P., Zhu, X.F., 2011a. Selective fast pyrolysis of biomass impregnated with $ZnCl_2$ to produce furfural: analytical Py-GC/MS study. J. Anal. Appl. Pyrol. 90, 204–212.

Lu, Q., Yang, X.C., Dong, C.Q., Zhang, Z.F., Zhang, X.M., Zhu, X.F., 2011b. Influence of pyrolysis temperature and time on the cellulose fast pyrolysis products: analytical Py–GC/MS study. J. Anal. Appl. Pyrol. 92, 430–438.

Lu, Q., Zhang, X.M., Zhang, Z.F., Zhang, Y., Zhu, X.F., Dong, C.Q., 2012. Catalytic fast pyrolysis of cellulose mixed with sulfated titania to produce levoglucosenone: analytical Py–GC/MS study. Bioresources 7, 2820–2834.

Mohan, D., Pittman, C.U., Steele, P.H., 2006. Pyrolysis of wood/biomass for bio-oil: a critical review. Energy Fuel 20, 848–889.

Nowakowski, D.J., Woodbridge, C.R., Jones, J.M., 2008. Phosphorus catalysis in the pyrolysis behaviour of biomass. J. Anal. Appl. Pyrol. 83, 197–204.

Ohnishi, A., Kato, K., Takagi, E., 1975. Curie-point pyrolysis of cellulose. Polym. J. 7, 431–437.

Ranganathan, S., Macdonald, D.G., Bakhshi, N.N., 1985. Kinetic studies of wheat straw hydrolysis using sulphuric acid. Can. J. Chem. Eng. 63, 840–844.

Sarotti, A.M., Spanevello, R.A., Suarez, A.G., 2007. An efficient microwave-assisted green transformation of cellulose into levoglucosenone. Advantages of the use of an experimental design approach. Green Chem. 9, 1137–1140.

Sarotti, A.M., Zanardi, M.M., Spanevello, R.A., Suarez, A.G., 2012. Recent applications of levoglucosenone as chiral synthon. Curr. Org. Synth. 9, 439–459.

Shafizadeh, F., Chin, P.P.S., 1976. Pyrolytic production and decomposition of 1,6-anhydro-3,4-dideoxy-b-D-glycero-hex-3-enopyranose-2-ulose. Carbohydr. Res. 46, 149–154.

Shafizadeh, F., Furneaux, R.H., Stevenson, T.T., Cochran, T.G., 1978. Acid-catalyzed pyrolytic synthesis and decomposition of 1,4:3,6-dianhydro-α-D-glucopyranose. Carbohydr. Res. 61, 519–528.

Shen, D.K., Gu, S., 2009. The mechanism for thermal decomposition of cellulose and its main products. Bioresour. Technol. 100, 6496–6504.

Sui, X.W., Wang, Z., Liao, B., Zhang, Y., Guo, Q.X., 2012. Preparation of levoglucosenone through sulfuric acid promoted pyrolysis of bagasse at low temperature. Bioresour. Technol. 103, 466–469.

Wang, S., Guo, X., Liang, T., Zhou, Y., Luo, Z., 2012. Mechanism research on cellulose pyrolysis by Py–GC/MS and subsequent density functional theory studies. Bioresour. Technol. 104, 722–728.

Wang, S., Guo, X., Wang, K., Luo, Z., 2011a. Influence of the interaction of components on the pyrolysis behavior of biomass. J. Anal. Appl. Pyrol. 91, 183–189.

Wang, Z., Lu, Q., Zhu, X.F., Zhang, Y., 2011b. Catalytic fast pyrolysis of cellulose to prepare levoglucosenone using sulfated zirconia. ChemSusChem 4, 79–84.

Wei, X., Wang, Z., Wu, Y., Yu, Z., Jin, J., Wu, K., 2014. Fast pyrolysis of cellulose with solid acid catalysts for levoglucosenone. J. Anal. Appl. Pyrol. 107, 150–154.

Zandersons, J., Zhurinsh, A., Dobele, G., Jurkjane, V., Rizhikovs, J., Spince, B., Pazhe, A., 2013. Feasibility of broadening the feedstock choice for levoglucosenone production by acid pre-treatment of wood and catalytic pyrolysis of the obtained lignocellulose. J. Anal. Appl. Pyrol. 103, 222–226.

Zhang, H., Xiao, R., Jin, B., Xiao, G., Chen, R., 2013. Biomass catalytic pyrolysis to produce olefins and aromatics with a physically mixed catalyst. Bioresour. Technol. 140, 256–262.

Zhang, Z.B., Lu, Q., Ye, X.N., Xiao, L.P., Dong, C.Q., Liu, Y.Q., 2014. Selective production of phenolic-rich bio-oil from catalytic fast pyrolysis of biomass: comparison of $K_3PO_4$, $K_2HPO_4$, and $KH_2PO_4$. Bioresources 9, 4050–4062.